

# Dynamical Synapses Causing Self-Organized Criticality in Neural Networks

A. Levina<sup>1,2,3</sup>, J. M. Herrmann<sup>1,4</sup>, T. Geisel<sup>1,3,4</sup>

<sup>1</sup>Bernstein Center for Computational Neuroscience Göttingen

<sup>2</sup>Graduate School “Identification in Mathematical Models”

<sup>3</sup>Max Planck Institute for Dynamics and Self-Organization

<sup>4</sup>Department of Physics, Georg-August University Göttingen  
Bunsenstr. 10, 37073 Göttingen, Germany

February 9, 2022

Self-organized criticality [1] is one of the key concepts to describe the emergence of complexity in natural systems. The concept asserts that a system self-organizes into a critical state where system observables are distributed according to a power-law. Prominent examples of self-organized critical dynamics include, e.g., piling of granular media [2], plate tectonics [3] and stick-slip motion [4]. Critical behavior has been shown to bring about optimal computational capabilities [5], optimal transmission [6] and storage of information [7], and sensitivity to sensory stimuli [8, 9, 10]. In neuronal systems the existence of critical avalanches was predicted in a paper of one of the present authors [11] and observed experimentally by Beggs and Plenz [6, 12, 13]. Nevertheless, while in the experiments critical avalanches were found generically in the sense of genuine self-organized criticality, in the model of Ref. [11] they only show up, if the set of parameters is fine-tuned externally to a critical transition state. In the present paper we demonstrate analytically and numerically that by assuming (biologically more realistic) dynamical synapses [14] in a spiking neural network, the neuronal avalanches turn from an exceptional phenomenon into a typical and robust self-organized critical behavior if the total resources of neurotransmitter are sufficiently large.

In multi-electrode recordings on slices of rat cortex and neuronal cultures [6, 12] neuronal avalanche were observed whose sizes were distributed according to a power-law with an exponent of  $-3/2$ . The distribution was stable over a long period of time. Variations of the dynamical behavior are induced by application or wash-out of neuromodulators. Qualitatively identical behavior can be reached in models like [11, 15] by variations of a global connectivity parameter. In these models, criticality only shows up, if the interactions are fixed precisely at a specific value or connectivity structure.

Here we study a model with activity-dependent depressive synapses and show that existence of several dynamical regimes can be reconciled with parameter-independent criticality. We find that synaptic de-

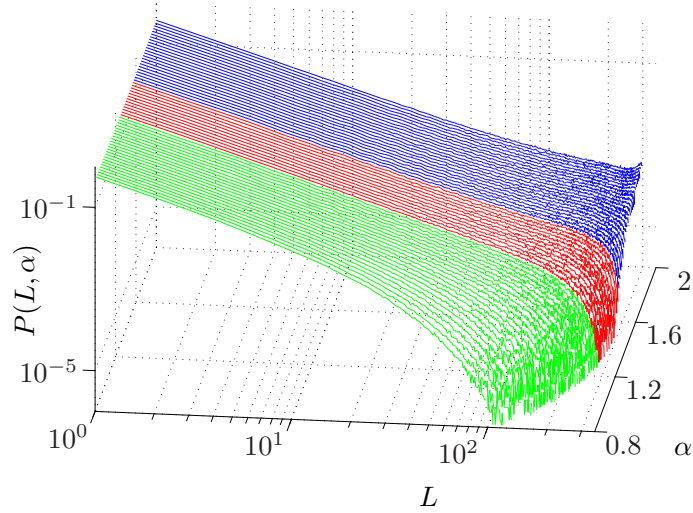


Figure 1: Distribution of avalanche sizes for different coupling strengths  $\alpha$ . At  $\alpha < 1.3$  small avalanches are preferred yielding a subcritical distribution. The range of connectivity parameters near  $\alpha = 1.4$  appears critical. For  $\alpha > 1.6$  the distribution is supercritical, i.e. a substantial fraction of firing events spreads through the whole system. These results are shown for  $N = 300$ ,  $\nu = 10$ ,  $u = 0.2$ ,  $I^{\text{ext}} = 0.025$ , other parameter values are discussed below.

pression causes the mean synaptic strengths to approach a critical value for a certain range of interaction parameters, while outside this range other dynamical behaviors are prevalent, cf. Fig. 1. We analytically derive an expression for the average coupling strengths among neurons and the average inter-spike intervals in a mean-field approach. The mean field approximation is applicable here even in the critical state, because the quantities that are averaged do not exhibit power-laws, but unimodal distributions. These mean values obey a self-consistency equation which allows us to identify the mechanism that drives the dynamics of the system towards the critical regime. Moreover, the critical regime induced by the synaptic dynamics is robust to parameter changes.

Consider a network of  $N$  integrate-and-fire neurons. Each neuron is characterized by a membrane potential  $0 < h_i(t) < \theta$ . The neurons receive external inputs by a random process  $\xi_\tau \in \{1, \dots, N\}$  which selects a neuron  $\xi_\tau(t) = i$  at a rate  $\tau$  and advances the membrane potential  $h_i$  by an amount  $I^{\text{ext}}$ . Each neuron integrates inputs until it reaches a threshold  $\theta$ . As soon as  $h_i(t) > \theta$  the neuron emits a spike which is delivered to all postsynaptic neurons at a fixed delay  $\tau_d$ . The membrane potential is reset by  $h_i(t_{\text{sp}}^+) = h_i(t_{\text{sp}}) - \theta$ . For simplicity we will assume in the following that  $\theta = 1$ . Super-threshold activity is communicated along neural connections of a strength proportional to  $J_{ij}$  to other neurons and may cause them to fire. In this way an avalanche of neural activity of size  $L \geq 1$  is triggered. More precisely, an avalanche is a period of activity that is initiated by an external input and that terminates when no further neuron becomes activated. We define the size of the avalanche as the number of participating

neurons. The dynamics of the membrane potential is described by the following equation

$$\dot{h}_i = \delta_{i,\xi_\tau(t)} I^{\text{ext}} + \frac{1}{N} \sum_{j=1}^N u J_{ij} \delta(t - t_{\text{sp}}^j - \tau_d). \quad (1)$$

In studies of self-organized criticality typically a separation of time scales is assumed which enters in Eq. 1 by the condition  $\tau_d \ll \tau$ . It allows us to assume that external input is absent during avalanches. Later, in the discrete version of the model,  $\tau$  will play the role of the temporal step size. The variables  $J_{ij}$  are subject to the dynamics

$$\dot{J}_{ij} = \frac{1}{\tau_J} \left( \frac{\alpha}{u} - J_{ij} \right) - u J_{ij} \delta(t - t_{\text{sp}}^j), \quad (2)$$

which describes the amount of available neurotransmitter in the corresponding synapse [14]. Namely, if a spike arrives at the synapse, the available transmitter is diminished by a fraction  $u$ , i.e. the synaptic strength decreases due to the usage of transmitter resources. If the presynaptic neuron is silent then the synapse recovers and its strength  $J_{ij}$  approaches the value  $\alpha/u$  at a slow time scale  $\tau_J = \tau\nu N$  with  $1 < \nu \ll N$ . Thus, the maximal strength of a connection is determined by the parameter  $\alpha$  and can be observed only when the synapse is fully recovered. The behavior of the network is determined, however, by the averaged synaptic strength which will be denoted by  $\langle J_{ij} \rangle$  with the average taken with respect to the distribution of inter-spike intervals. In order to obtain our main result we will calculate this effective value and use it in a static network. The uniform strengths of the static network are denoted by  $\alpha_0$ .

If the external drive and the synaptic weights are small, the activity of the network consists of short burst-like events which are initiated by a particular external input. The firing events are separated by relatively long relaxation intervals when external inputs are integrated. We may thus be tempted to assume  $J \approx \frac{\alpha}{u}$  before any spiking event. In general, however, we must take into account that the efficacy of a synapse varies in a usage-dependent way which compensates large levels of network activity. Depending on the synaptic strength the network can produce a rich repertoire of behaviors. In Fig. 1, we show examples of avalanche size distributions for various values of  $\alpha$ . For small values of  $\alpha$ , subcritical avalanche-size distributions are observed. This regime is characterized by a negligible number of avalanches that extend to the system size. Near  $\alpha_{\text{cr}}$  the system has an approximate power-law avalanche distribution for avalanche sizes almost up to the system size where an exponential cut-off is observed. The mean-squared deviation from an exact power law is shown in Fig. 2. Finally, the distribution of avalanche sizes becomes non-monotonous when  $\alpha$  is well above the critical value  $\alpha_{\text{cr}}$ .

In preliminary numerical studies we had assumed a model with facilitating and depressing synapses [17]. Here we conclude that facilitating synapses are not necessary to evoke self-organized critical avalanches in spiking neural networks, depressing synapses are sufficient. This is in line with the observation [18] that synapses that connect excitatory neurons are largely depressive. To identify the parameters of the avalanche size distribution it is sufficient to determine the average synaptic strength: As seen in Fig. 3 both the power-law exponent and the mean-squared deviation from the power-law are the same for networks with dynamical synapses and networks with static synapses if the strength of the static synapses is chosen as  $\alpha_0 = u \langle J_{ij} \rangle$ . In order to calculate the average synaptic strength analytically, we consider in addition the neural inter-spike intervals  $\Delta^{\text{isi}}$ . On the one hand, if the inter-spike intervals are short then the synapses have a short time to recover and the average synaptic strength resides at a low level. On the other hand, large synaptic strengths lead to long avalanches and to large input to neurons during the avalanches, which tends to shorten the inter-spike intervals.

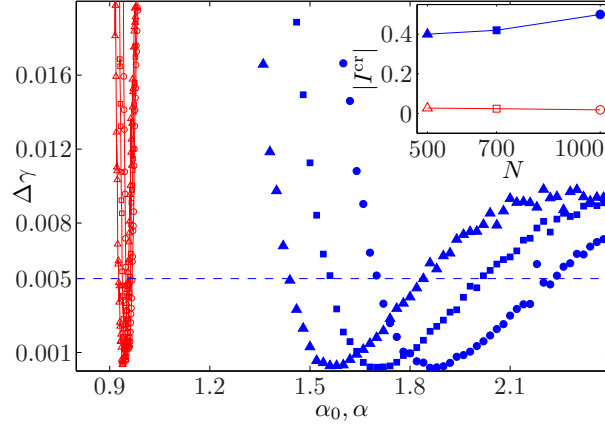


Figure 2: The range of connectivity parameters which cause a critical dynamics extends with system size. The mean-squared deviation from the best-matching power-law is plotted in dependence of the connection strengths  $\alpha_0$  and  $\alpha$  for static synapses and depressive synapses, respectively. Blue circles, squares and triangles stand for networks with dynamical synapses and system sizes  $N = 1000$ ,  $700$ , and  $500$ , respectively. Red symbols represent the static model. Note that the minimum of all curves depends of the network size [11]. The inset (same symbols) shows the lengths of the parameter intervals where the deviation from the best-matching power-law is smaller than an ad-hoc threshold ( $\Delta\gamma = 0.005$ ).

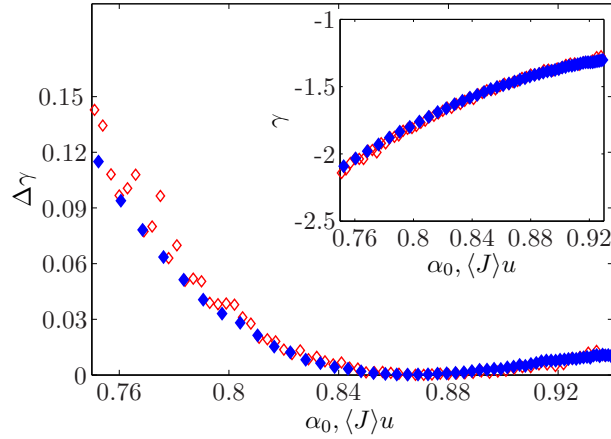


Figure 3: Rescaling of depressive synapses. A network with static synapses of uniform strength  $\alpha_0$  has the same statistical properties as a network with dynamic synapses if  $\alpha_0$  is fixed at the average synaptic strength of the dynamical case, i.e. if  $\alpha_0 := \langle J \rangle u$ . The mean-squared deviation  $\Delta\gamma$  from the best-matching power-law is shown as a function of the synaptic strength  $\alpha_0$  for static synapses (red symbols) and the mean synaptic strength for dynamical synapses (blue symbols), respectively. The inset (same symbols) shows the exponent  $\gamma$  of the best-matching power-law in the two cases. Parameters are  $N = 100$ ,  $\nu = 10$ ,  $u = 0.2$ .

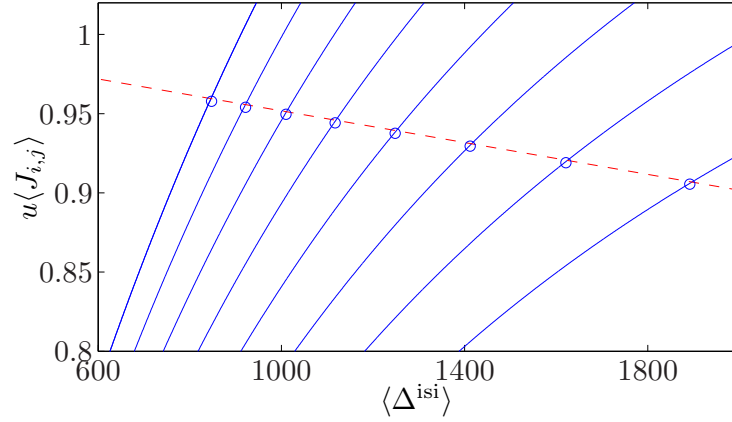


Figure 4: The graphical solution of Eqs. 3 establishes a functional relation between the average synaptic strength and inter-spike interval. It is obtained by the intersections of the solutions of Eq. 12 (dashed line) and Eq. 7 (solid lines) for  $\alpha = 1.3, \dots, 2.0$  in steps of 0.1 (from right to left). This solution agrees well with the results of simulations (circles) of a network with the same values of  $\alpha$ . Parameters are  $N = 500$ ,  $\nu = 10$ ,  $u = 0.2$ .

This trade-off determines the expected values of the synaptic strengths and the inter-spike intervals which are realized by the dynamics of the network. In order to express this reasoning more formally, we solve the dynamical equations (1) and (2) based on a stationarity assumption for both the synaptic strengths and the inter-spike interval. Neither of these quantities has a power-law distribution and their first moments exist. In **Methods** we derive expressions of the mean synaptic strength  $\langle J_{ij} \rangle$  and the mean value of the inter-spike intervals distribution  $\langle \Delta^{\text{isi}} \rangle$ . The stochastic dependency of the two quantities is reflected in a mutual dependence of their averages. Each of the dependencies is derived analytically which allows us to formulate the self-consistency of the stationarity requirement as the simultaneous solution of the mean-field equations

$$\langle J_{ij} \rangle = \langle J_{ij} \rangle \left( \langle \Delta^{\text{isi}} \rangle \right) \quad \text{and} \quad \langle \Delta^{\text{isi}} \rangle = \langle \Delta^{\text{isi}} \rangle \left( \langle J_{ij} \rangle \right) \quad (3)$$

which can be determined graphically from the intersections of the solutions of Eqs. 7 and 12, cf. Fig. 4. The mean-field solution is confirmed by direct network simulations that are represented by the circles in Fig. 4. The solution is unique for any  $\alpha$ . The stationary distribution is less sensitive to changes of the parameter  $\alpha$  near the critical value of the synaptic strength than further away from it. This brings about the large critical region for the model with depressive synapses, cf. Fig. 2.

Furthermore we want to discuss the stability of the solution of the self-consistency equation (3). If we apply a perturbation  $\Delta J$  to all synapses at time  $t_p$  such that for each  $i, j$   $\widetilde{J}_{ij} = J_{ij} + \Delta J$ , we can show with some simple computations, that before the next spike the synaptic strengths are on average smaller than  $\widetilde{J}_{ij}$ . In the simulated system the average synaptic strength is driven back to the fixed point by a few spikes, such that the solution of (3) is indeed stable for the critical state.

Both the numerical study in Ref. [17] and the analysis presented so far refer to finite systems. In order to check whether the trend that is visible in Fig. 2 continues for larger network sizes, we consider the

behavior of the mean synaptic strength in the thermodynamic limit  $N \rightarrow \infty$  we compute the expectation value of the avalanche-size distribution (11),  $\langle L \rangle = \frac{N}{N-(N-1)\alpha_0}$  [11], and insert it into the self-consistency equation (3)

$$\frac{\alpha \left(1 - e^{-\frac{1}{\nu N} \langle \Delta^{\text{isi}} \rangle}\right)}{1 - (1-u)e^{-\frac{1}{\nu N} \langle \Delta^{\text{isi}} \rangle}} = \frac{N}{N-1} - \frac{I^{\text{ext}} \langle \Delta^{\text{isi}} \rangle}{N-1}. \quad (4)$$

In the limit  $N \rightarrow \infty$  we should scale the external input  $I^{\text{ext}} \sim N^{-w}$  and  $w > 0$ . We now distinguish the following cases. a) If  $\langle \Delta^{\text{isi}} \rangle \sim N^{1+\epsilon}$  and  $\epsilon > w$  then the right hand side (r.h.s.) of (4) tends to  $-\infty$ , while the l.h.s. is always larger than 0. b) If  $\langle \Delta^{\text{isi}} \rangle \sim N^{1+\epsilon}$  and  $0 < \epsilon \leq w$  then the r.h.s. of (4) tends to 1 (or 0 if  $\epsilon = w$ ) while the l.h.s.  $\alpha$ , hence a solution is only possible if  $\alpha = 1$  and in this case  $u \langle J_{ij} \rangle \rightarrow 1$ . c) If  $\langle \Delta^{\text{isi}} \rangle \sim N^{1-\epsilon}$  and  $\epsilon < 0$  then the r.h.s. of (4) tends to 1, while the l.h.s. approaches 0. d) If  $\langle \Delta^{\text{isi}} \rangle \sim N$ , we can assume that  $\langle \Delta^{\text{isi}} \rangle = cN + o(N)$ . From (4) for  $\alpha > 1$  we can find the unique solution  $c = -\nu(\ln(\alpha-1) - \ln(\alpha-1+u))$ . In all cases when the solution exists,  $u \langle J_{ij} \rangle \rightarrow 1$ , which we know to be the critical connectivity for the network with statical synapses in the limit  $N \rightarrow \infty$ . Hence in the thermodynamical limit the network with dynamical synapses becomes critical for any  $\alpha \geq 1$ .

In this paper we have focused on fully connected networks and neurons without leak currents for reasons of analytical tractability. We now discuss the results of various generalizations which we have investigated numerically. If the network has only partial connectivity, the results stay the same, if the synaptic strengths are properly rescaled. In a random network of size  $N$  with connectivity probability  $c$ , the critical parameter  $\alpha$  is approximately equal to  $\alpha_N^{\text{cr}}/c$ , where  $\alpha_N^{\text{cr}}$  is obtained from the critical parameter region of the fully connected network of size  $c \times N$ . If the connections in a partially connected random network are not chosen independently (e.g. “small-world” connectivity [19]) one finds even more accurate power-laws than for the independent case with the same average connectivity. A similar phenomenon occurs in the grid network [16] which has been used to model criticality in EEG recordings.

If in Eq. 1 we add a leak term, which is present in biologically realistic situations

$$\dot{h}(t) = -\tau_l^{-1}h(t) + C + \delta_{i,\xi_\tau(t)}I^{\text{ext}} + \frac{1}{N} \sum_{j=1}^N u J_{ij} \delta(t - t_{\text{sp}}^j - \tau_d), \quad (5)$$

we find numerically that the distribution of the avalanche sizes remains a power law for leak time-constants up to  $\tau_l \approx 40\text{ms}$ . In (5) we included a constant compensatory synaptic current  $C$  which depends on  $\tau_l$  and summarizes neuronal self-regulatory mechanisms. In this way the probability of the neuron to stay near threshold is conserved and avalanches are triggered in a similar way as in the non-leaky case. The resulting power-law exponent is slightly smaller than  $-1.5$  and reaches values close to  $-2$  for strong leakage in simulations of a network of  $N = 500$  neurons.

In summary, we have presented an analytical and numerical study of spiking neural networks with dynamical synapses. Activity-dependent synaptic regulation leads to the self-organization of the network towards a critical state. The analysis demonstrates that mean synaptic efficacy hereby plays a crucial role. We explained how the critical state depends on the maximally available resources and have shown that in the thermodynamic limit the network becomes critical for any  $\alpha \geq 1$ , i.e. that criticality is an intrinsic phenomenon produced by the synaptic dynamics. The mean field quantities are in very good agreement with simulations and were shown to be robust with respect to perturbations of the model parameters.

**Acknowledgments:** We thank Manfred Denker and Tomoki Fukai for useful discussions. This work was partially supported by the BMBF in the framework of the Bernstein Centers for Computational Neuroscience, grant number 01GQ0432. A.L. has received support from DFG Graduiertenkolleg N1023.

## Methods

In this section we give an explicite derivation of the self-consistency relation (3). Solving Eq. 2 between two spikes of neuron  $j$  we find

$$J_{ij}(t_2^-) = \frac{\alpha}{u} \left( 1 - \left( 1 - \frac{u}{\alpha} J_{ij}(t_1^+) \right) e^{-(t_2-t_1)/\tau_J} \right), \quad (6)$$

where the synaptic strengths immediately before and after a spike of neuron  $j$  at time  $t_s$  are denoted by  $J_{ij}(t_s^-)$  and  $J_{ij}(t_s^+)$ , respectively. Within a short interval containing the spike,  $J_{ij}$  decreases by a fraction  $u$  such that  $J_{ij}(t_1^+) = (1-u) J_{ij}(t_1^-)$ .

The average synaptic strength  $\langle J_{ij} \rangle$  is the expectation value of  $J_{ij}(t_s^-)$ . Analogously,  $\langle \Delta^{\text{isi}} \rangle$  refers to the inter-spike interval  $\Delta^{\text{isi}}$ . The random variables  $J_{ij}(t_s^-)$  and  $\Delta^{\text{isi}}$  both depend on the distribution of external inputs and are thus related. The self-consistency conditions (3) express this relation for the respective averages. Assuming that  $\langle J_{ij} \rangle$  depends essentially only on the mean inter-spike interval, we obtain from (6):

$$\langle J_{ij} \rangle = \frac{\alpha}{u} \frac{1 - e^{-\frac{1}{\nu N} \langle \Delta^{\text{isi}} \rangle}}{1 - (1-u)e^{-\frac{1}{\nu N} \langle \Delta^{\text{isi}} \rangle}}, \quad (7)$$

where the average is performed in discrete time with step width  $\tau$ , i.e.  $\tau_J = \nu N$ .

We are now going to establish a relation between  $P(\Delta^{\text{isi}})$  and the inter-avalanche interval distribution  $Q(\Delta^{\text{iai}})$ . It can be shown that the neuronal membrane potentials before an avalanche are uniformly distributed on the interval  $[\epsilon_N, \theta]$ , where  $\epsilon_N$  is a lower bound of  $h_i(t_{\text{sp}}) - \theta$  with  $\epsilon_N \rightarrow 0$  for  $N \rightarrow \infty$ . Under these conditions,  $Q(\Delta^{\text{iai}})$  has a geometric distribution

$$Q(\Delta^{\text{iai}}) = \frac{I^{\text{ext}}}{\theta - \epsilon_N} \left( 1 - \frac{I^{\text{ext}}}{\theta - \epsilon_N} \right)^{\Delta^{\text{iai}}}. \quad (8)$$

Let  $k_j$  be the number of avalanches between two spikes of the neuron  $j$ . A mean-field approximation relates the averages of the distributions of inter-spike and inter-avalanche intervals

$$\langle \Delta^{\text{isi}} \rangle = \langle k \rangle \langle \Delta^{\text{iai}} \rangle. \quad (9)$$

The average inter-avalanche interval is easily computed from (8)

$$\langle \Delta^{\text{iai}} \rangle = \frac{\theta - \epsilon_N}{I^{\text{ext}}}. \quad (10)$$

In order to calculate the average number of avalanches between two spikes of a neuron, we compute the time to reach the threshold by accumulating external inputs and spikes from other neurons during avalanches, i.e.

$$\langle \kappa \rangle = \frac{\theta}{u \langle J_{ij} \rangle \langle L \rangle + I^{\text{ext}} \frac{\langle \Delta^{\text{iai}} \rangle}{N}},$$

where  $\langle L \rangle$  is the mean avalanche size and  $\frac{1}{N}$  is the probability that neuron  $j$  is receiving an input. The distribution of avalanche sizes can be computed analytically for a network with static synapses of strength  $\alpha_0$  [11]:

$$P(L, \alpha_0, N) = L^{L-2} \binom{N-1}{L-1} \left( \frac{\alpha_0}{N} \right)^{L-1} \left( 1 - L \frac{\alpha_0}{N} \right)^{N-L-1} \frac{N(1-\alpha_0)}{N - (N-1)\alpha_0}. \quad (11)$$

In the case of dynamical synapses we apply a mean field approximation and set  $\alpha_0 = u \langle J_{ij} \rangle$  in (11). This allows us to compute  $\langle L \rangle$  as a function of  $(u \langle J_{ij} \rangle)$ .

Combining (9), (10), and (11) we obtain a relation between the inter-spike interval and the average synaptic strength.

$$\langle \Delta^{\text{isi}} \rangle = \frac{\theta - \epsilon_N}{I_{\text{ext}}} \frac{\theta}{u \langle J_{ij} \rangle \langle L \rangle (u \langle J_{ij} \rangle) + I_{\text{ext}} \frac{\theta - \epsilon_N}{N}}. \quad (12)$$

The self-consistency equations (3) arise from (7) and (12). Its solution is obtained by numerical analysis of the two independent relations (7) and (12), cf. Fig. 4.

## References

- [1] P. Bak, C. Tang, and K. Wiesenfeld. Self-organized criticality: An explanation of the 1/f noise. *Phys. Rev. Lett.* **59**, 381–384, (1987).
- [2] V. Frette, K. Christensen, A. M. Mølten-Sørensen, J. Feder, T. Jøssang, and P. Meakin. Avalanche dynamics in a pile of rice. *Nature* **397**, 49–52, (1996).
- [3] B. Gutenberg and C. F. Richter. Magnitude and energy of earthquakes. *Annali di Geofisica* **9**, 1–15, (1956).
- [4] H. J. S. Feder and J. Feder. Self-organized criticality in a stick-slip process. *Phys. Rev. Lett.* **66**, 2669–2672, (1991).
- [5] R. A. Legenstein, W. Maass. Edge of chaos and prediction of computational performance for neural microcircuit models. *Neural Networks*, 323–333(2007).
- [6] J. Beggs and D. Plenz. Neuronal avalanches in neocortical circuits. *J. Neurosci.* **23**, 11167–11177, (2003).
- [7] C. Haldeman and J. Beggs. Critical branching captures activity in living neural networks and maximizes the number of metastable states. *Phys. Rev. Lett.* **94**, 058101, (2005).
- [8] R. Der, F. Hesse, and G. Martius. Rocking stumper and jumping snake from a dynamical system approach to artificial life. *Adaptive Behavior*. **14**(2): 105–115, (2006) .
- [9] O. Kinouchi, M. Copelli. Optimal dynamical range of excitable networks at criticality. *Nature Physics* **2**, 348–352, (2006).
- [10] D. Chialvo. Are our senses critical? *Nature Physics* **2**, 301–302, (2006).
- [11] C. W. Eurich, M. Herrmann, and U. Ernst. Finite-size effects of avalanche dynamics. *Phys. Rev. E* **66**, 066137-1-15, (2002).



- 
- [12] J. Beggs and D. Plenz. Neuronal avalanches are diverse and precise activity patterns that are stable for many hours in cortical slice cultures. *J. Neurosci.* **24**:22, 5216–5229, (2004).
  - [13] D. Plenz, T. C. Thiagarajan. The organizing principles of neuronal avalanches: cell assemblies in the cortex? *Trends in Neurosciences*, **30** 3, 101–110, (2007)
  - [14] H. Markram and M. Tsodyks. Redistribution of synaptic efficacy between pyramidal neurons. *Nature* **382**, 807–810, (1996).
  - [15] J. Teramae, T. Fukai. Local cortical circuit model inferred from power-law distributed neuronal avalanches. *J Comput Neurosci*, **22**(3), 301–312, (2007).
  - [16] L. de Arcangelis, C. Perrone-Capano, H. J. Herrmann. Self-organized criticality model for brain plasticity *Phys. Rev. Lett.* **96**, 028107(4), (2006).
  - [17] A. Levina, J. M. Herrmann, T. Geisel. Power-law distribution of neuronal avalanches. *Proc. 19th Annual Conference on Neural Information Processing Systems*, editors: Y. Weiss, B. Schölkopf, and J. Platt, MIT Press, 771–778, (2006).
  - [18] M. Tsodyks, K. Pawelzik, and H. Markram. Neural networks with dynamic synapses. *Neural Computation* **10**, 821–835, (1998).
  - [19] M. Lin, T.-L. Chen. Self-organized criticality in a simple model of neurons based on small-world networks. *Phys. Rev. E* 71, 016133 (2005)